Materials Chemistry and Physics 233 (2019) 236–241

Contents lists available at ScienceDirect

Materials Chemistry and Physics

journal homepage: www.elsevier.com/locate/matchemphys

The using of thermal analysis methods for study of pore formation in the system resol phenol-formaldehyde resin – Ethylene glycol – *p*-toluenesulfonyl chloride

M.A. Khaskov *, A.I. Gulyaev, S.D. Sinyakov, S.A. Ponomarenko

All-Russian Scientific Research Institute of Aviation Materials, Russian Federation, 105005, Moscow, Radio Str., Bld.17, Russia

ARTICLE INFO

Keywords:
Porous carbon matrix
Polymerization induced phase separation
Thermal analysis
Thermoporometry
Scanning electron microscopy
Phenol-formaldehyde resin

ABSTRACT

The pore formation in the system resol resin – ethylene glycol – *p*-toluenesulfonyl chloride based on polymerization induced phase separation (PIPS), post-curing and pyrolysis techniques are studied by thermal analysis methods, pyrolysis gas chromatography mass spectrometry and electron microscopy. The presence of *p*-toluenesulfonyl chloride leads to accelerating of curing reaction and reaction order increasing. It was shown that PIPS step determines the texture and morphology of final carbon matrix precursors. The increasing of PIPS step temperature results in decreasing of the segregation scale and increasing of segregation intensity of phase separation. The decreasing of PIPS step temperature leads to increasing of macropores sizes, but decreasing of mesopores cumulative volumes. The increased mesopores content at high PIPS temperature is supposed to be resulted and from the oligoethylene glycol formation. Insufficient PIPS step time leads to partial collapsing of formed porous structure during pyrolysis.

1. Introduction

The ceramic matrix composites (CMCs) are widely used nowadays as the structural materials under the conditions of corrosive and oxidative atmosphere, temperature cycling and thermal shock [1,2]. There are many methods of CMCs manufacture such as chemical vapor infiltration [3], use of polymer-derived ceramics, sol-gel processing [4,5] and others with their advantages and disadvantages [6]. The reactive melt infiltration has outstanding advantages over traditional ceramic processing methods which include relatively low temperature of manufacturing and ability to form complex near-net final shapes and to achieve zero or low porosity [7]. In the case of carbide-forming reactive melts such as silicon based alloys, the initial carbon preforms should have sufficient open porosity and permeability to achieve the uniform distribution of reactive melts before carbide formation. There are many methods to obtain the porous carbon matrix, for example, using the thermosetting matrix-precursors and pore-forming substances [8,9], different templates [10,11], directed crystallization [12] and many others. Polymerization induced phase separation (PIPS) is quite convenient tool for pore formation where non-reactive reagents in reactive monomer during polymerization create the domains resulting in voids after pyrolysis. Since PIPS depends on thermodynamic, kinetic and viscoelastic factors [13], different structures and morphologies can be obtained by changes of the components nature, their concentrations and polymerization time-temperature conditions. One of the promising systems for creation of porous carbon matrix is phenol-formaldehyde resin and ethylene glycol. There are many works concerning formation of porous carbon matrix in this system [14,15] including verified mathematical modeling of PIPS [16], but they regard only the characterization of the final products. The investigations of the intermediate products and the processes by different methods including thermal analysis can not only optimize the synthesis conditions, but improve the materials engineering at general. This work is devoted to study of pore formation in the system resol phenol-formaldehyde resin – ethylene glycol – *p*-toluenesulfonyl chloride by electron microscopy, pyrolysis gas chromatography mass spectrometry and thermal analysis methods.

2. Experimental

2.1. Materials

The resol phenol-formaldehyde (RPF) resin synthesized from phenol (99%, ACROS ORGANICS) and paraformaldehyde (90%, ACROS ORGANICS) in the presence of NaOH (molar ratio of Phenol/

* Corresponding author.
E-mail address: khaskov@mail.ru (M.A. Khaskov).

https://doi.org/10.1016/j.matchemphys.2019.05.060
Received 4 February 2019; Received in revised form 29 April 2019; Accepted 22 May 2019
Available online 24 May 2019

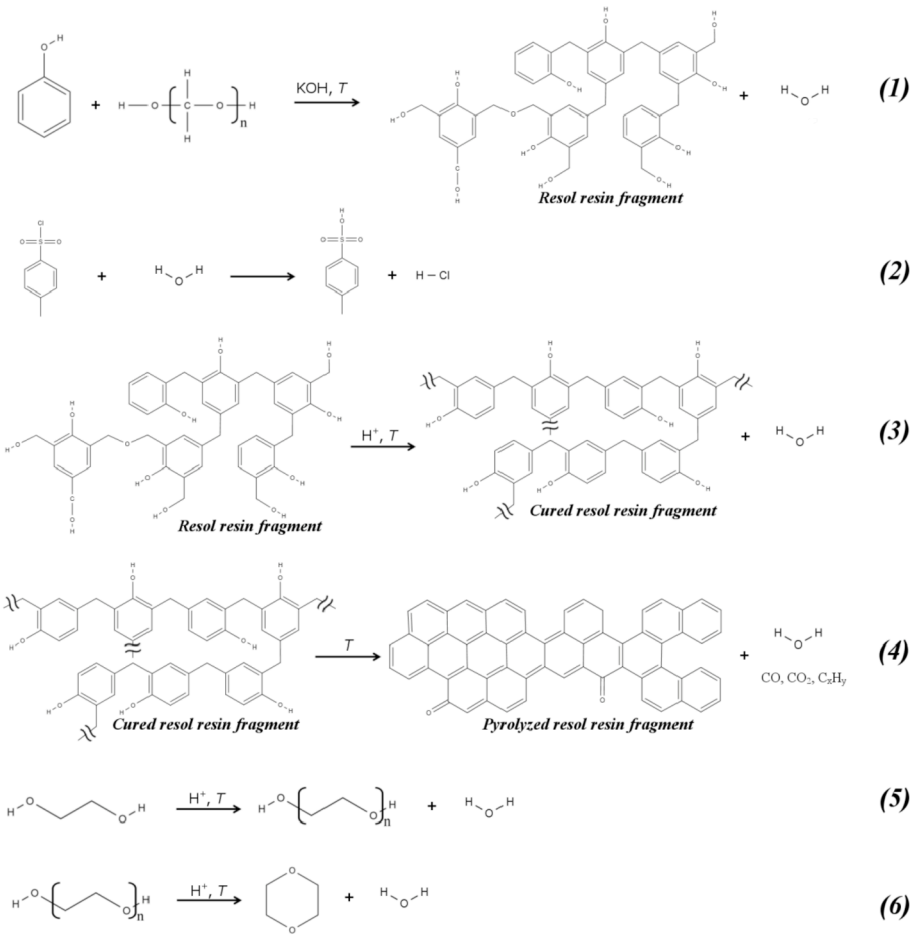

Fig. 1. The reaction mechanisms in the system investigated: 1 – resol resin synthesis, 2 – acid catalyst formation, 3 – resol resin curing, 4 – cured resol resin pyrolysis, 5 – ethylene glycol acid-catalyzed polycondensation, 6–1,4-dioxane formation.

Formaldehyde/NaOH = 1/1,7/0,024), ethylene glycol (99+%, ACROS ORGANICS) and *p*-toluenesulfonyl chloride (99+%, ACROS ORGANICS) were used as initial reagents.

2.2. Synthesis

2.1 g of *p*-toluenesulfonyl chloride were added to 20 g of ethylene glycol and stirred for 5 min. Then 20 g of RPF were added and stirred for 10 min by shaking. The composition obtained was denoted as FET1105. 10 g of FET1105 were put to the test-tube of geltimer GelNorm and inserted into the gel-timer furnace. After the gelation the sample were held at the same furnace until 8 h had reached. The samples after PIPS steps were denoted as FET1105-X, where X is the PIPS temperature (50, 60 or 70 °C). After the PIPS step the initial homogenous liquid composition separates in two phases: liquid one which is denoted as L (ethylene glycol and the liquid co-products of resol resin polycondensation) and solid one which is denoted as S (the main product of composition curing). The post-curing was carried out at 180 °C for 6 h. The samples after post-curing were denoted as FET1105-X-180. As a reference sample, the pure resol resin was used, which was cured in two steps: at 90 °C for 8 h and at 180 °C for 6 h. The cured reference sample was denoted as RPF-90-180. The pyrolysis of the samples was carried out in the furnace under dynamic argon atmosphere (10 l/min) using chosen time-temperature program.

3. Characterization

The curing reaction was investigated on the STA 449 F3 Netzsch device in the high-pressure crucible at the heating rate of 10 K/min. The evolved gas analysis during pyrolysis was performed on STA 449 F3 Netzsch device connected with Bruker Tensor 27 IR-spectrometer. The pyrolysis gas chromatography mass spectrometry was carried out on GCMS-QP2010S (Shimadzu) chromate-mass-spectrometer with Double-Shot Pyrolyzer (PY-2020iD). The thermoporometry was carried out on DSC 204 F1 Netzsch device at the heating rate of 1 K/min in the sealed aluminum crucibles. The calibration of temperature was carried out with the using of In, Sn, Zn, Bi, CsCl and bi-distilled water. The calibration of DSC-signal was carried out with the using of sapphire calibration disk. ASTM E2041-08 [17] was used for kinetics calculation. The degree of cure (conversion degree or fraction reacted) was calculated in accordance with ASTM E2041-08.

4. Result and discussion

4.1. The study of curing

Since the curing of the phenol-formaldehyde resin is accompanied with low-molecular weight products evolution (reaction 3, Fig. 1) and the using of ordinary pierced crucible can result in artifacts on the DSC-curves [18], the high-pressure crucibles were used for thermal analysis measurements.

The addition of ethylene glycol to resol resin slows down significantly the curing reaction [19], but the presence of catalyst in the system shifts the curing process to the area of lower temperatures (Fig. 2A). Moreover, the presence of catalyst allows performing gelation in the system without mass loss, since the possible temperature of the synthesis

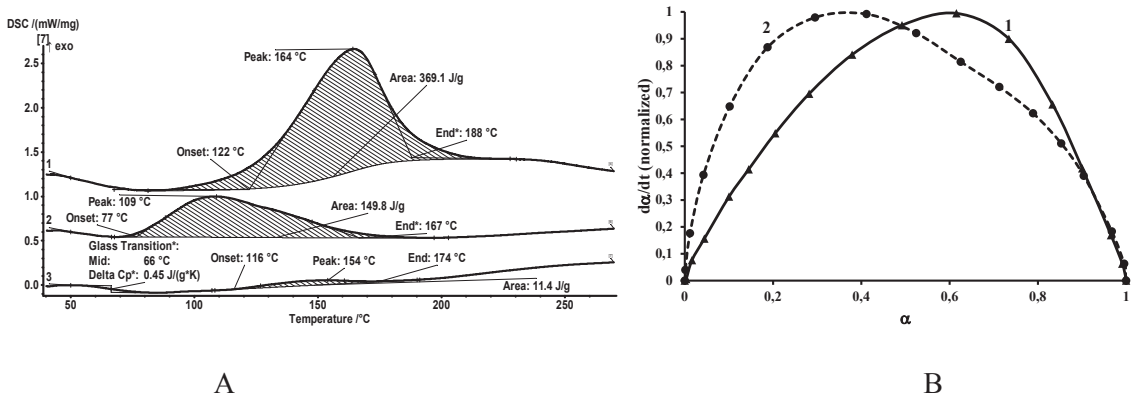

Fig. 2. A - DSC curves (A) and the dependence of dα/dt on α (B) for RPF (1) and FET1105 (2) and FET1105-60 (3).

is quite low to vaporize the product of polycondensation (water molecules) [19].

The FET1105 heat of cure is only 40 ± 4% of pure RPF resin, while the resol content in composition FET1105 is 48%. These observations directs on decreasing of cure degree of composition polymer network in composition in comparison with pure resol resin and about 15% of initial reactive groups do not participate in the curing reaction. Despite the fact that *p*-toluenesulfonyl chloride reacts easily with alcohols including phenols, this pathway of reactive groups (methylol groups in resol [20]) withdrawal should be excluded, since this reaction take place in the presence of base [21]. It should be mentioned, however, that according to Ref. [9], ethylene glycol in the phenol-formaldehyde system and the presence of pure formaldehyde can participate in curing mechanism resulting in –Ph-CH2-O-CH2-CH2-Ph-fragments formation.

According to Ref. [22], the curing kinetics of phenol-formaldehyde resins is best described as n-order model with the Borchardt–Daniels method (BD-method). The calculation of degree of cure (α) and reaction rate (dα/dt) were carried out using ASTM E2041-08. As one can see from the dependence of dα/dt on α (Fig. 2B), the presence of catalyst and ethylene glycol shifts the curve profile to the left. According to Ref. [23] such behavior can be related with increasing of reaction order.

4.2. The study of polymerization induced phase separation and post-curing products

The idea of pore formation in the chosen system is based on polymerization induced phase separation (PIPS) and the morphology and sizes of domains enriched with non-reactive compounds (ethylene glycol) should be dependent on the temperature. For example, the temperature influences the rate of thermoset component curing and, consequently, the thermodynamic factors of PIPS (enthalpy and entropy of demixing) change more rapidly with temperature increasing. The temperature also influences the mass transfer properties in the system and diffusion of components increases with increasing temperature. In accordance with morphology map of PIPS [24], the PIPS at higher temperature generally results in formation of the particles with smaller sizes, while polymerization induced phase separation at lower temperature leads to the particles with larger sizes. According to Ref. [25], the gelation and vitrification arrest the development of primary morphology during PIPS, while secondary phase separation can take place and after gelation. Nevertheless, the gel-point is critical time to formation of pore structure main morphology. However, according to Ref. [19], the final post curing at 180 °C of the composition immediately after gelation leads to the collapsing of the pores during pyrolysis and formation of the materials with density, which is nearly equal to initial uncured composition. It was suggested that gelation time is insufficient to form precursors that are structurally stable to pyrolysis. According to gelation measurements, the gel points of FET1105 are 20, 66 and 220 min at 70, 60 and 50 °C, respectively. According to Ref. [14] the developed pore structures after pyrolysis in the system phenol-formaldehyde resin – ethylene glycol – acid catalyst can be obtained after heat treatment at low temperature step (PIPS step) for 8 h. For example, the treatment of the sample FET1105 at 60 °C for 8 h leads to vitrification [26] of the polymer matrix (glass transition temperature is 66 °C, Fig. 2A) in FET-1105-60 sample and the reaching of conversion degree being equal to 92%.

Table 1
Some properties of RPF and FET1105 after PIPS, post-curing and pyrolysis steps.

Sample	m (PIPS), %	m (post-curing)[c], %	m (800 °C)[d], %	l_{800}/l_{25}[e]	ρ_{800}/ρ_{25}[f]
RPF	98[a]	82,8	65,3	0,197	1,1
FET1105	99 (95_s+4_l)[b]	63,7	42,2	0,242	0,6

[a] Residual mass after holding at 90 °C for 8 h (no PIPS).
[b] Residual mass after holding at 60 °C for 8 h, where 95 – residual mass of solid fraction and 4 – residual mass of liquid fraction (see experimental part).
[c] Residual mass after holding at 180 °C for 6 h.
[d] Residual mass after heating up to 800 °C under inert atmosphere (heating rate of 5 K/min).
[e] Linear shrinkage after heating up to 800 °C under inert atmosphere (heating rate of 5 K/min).
[f] The ratio of density at 800 °C to one at 25 °C before any heat treatment.

There are some mass loss and shrinkage of the samples during the PIPS and post-curing steps. The mass loss during the PIPS and post-curing steps of initial RPF and FET1105 are presented in Table 1. The PIPS step of FET1105 causes minor separation of visible solid (m_s) and liquid (m_l) fractions. As one can see from Table 1 the post-curing of initial phenol formaldehyde resin (RPF) is accompanied with mass loss of 17 wt %, which can be related with releasing of low molecular weight condensation products. On the other hand the post-curing of FET1105-60 solid fraction is accompanied with 36 wt% mass loss due to not only condensation products but non-RPF products (ethylene glycol, *p*-toluenesulfonyl chloride and their interaction products) as well. The linear shrinkage of the FET1105 sample during PIPS step and post-curing was negligible. The linear shrinkage of RPF after post-curing was about 2%. Thus, the density of RPF and FET1105 after PIPS steps (at 60 °C for FET1105 and at 90 °C for RPF) and post-curing decreased by 12 and 40%, respectively.

The structure forming step due to PIPS at different temperatures for 8 h and post-curing step at 180 °C for 6 h results in different morphology of the samples (Fig. 3) which is consistent with morphology map [24]: the lower temperature of PIPS the larger particle (pore) sizes in macroscale. The pores in the samples were formed due to removal of the domains enriched with ethylene glycol and other non-RPF products.

As can be seen from Fig. 3, there are quite uniform distribution of the pores in the samples, moreover the pores seems to have irregular forms.

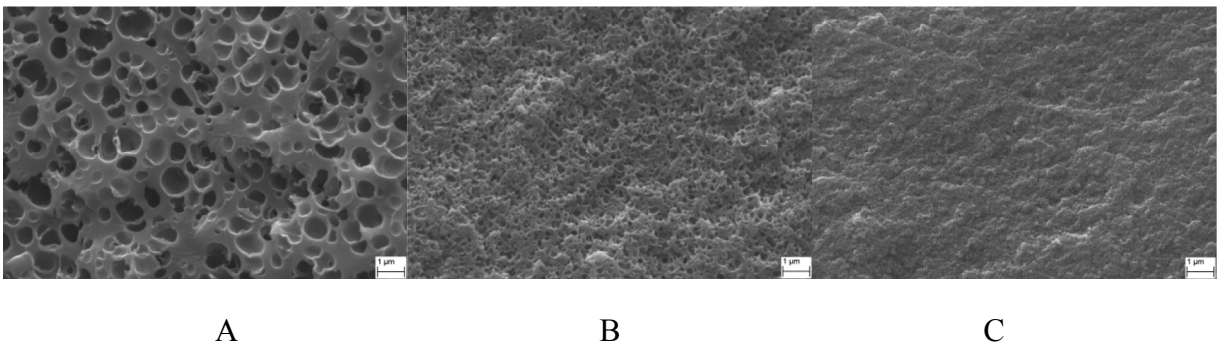

Fig. 3. Scanning electron microscopy images of the samples after post-curing (× 20000): A – PIPS at 50 °C (FET1105-50); B – PIPS at 60 °C (FET1105-60); C – PIPS at 70 °C (FET1105-70).

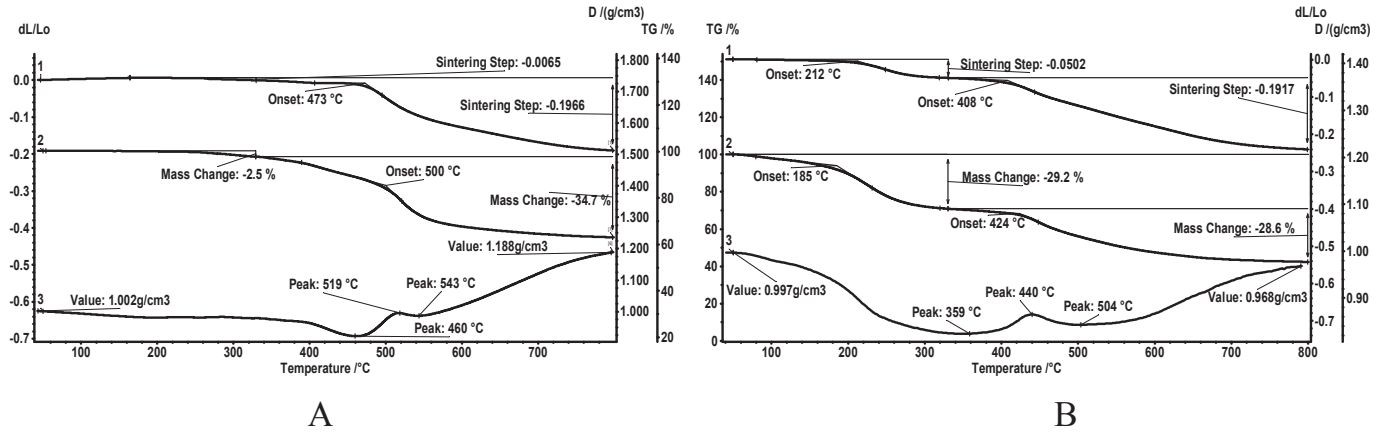

Fig. 4. The dependences of length (1), mass (2) and relative density (3) of the composition on the temperature during the heating under inert atmosphere of the samples: A – RPF-90-180, B - FET1105-60-180.

So it could be suggested, that PIPS in the system resol phenol-formaldehyde resin – ethylene glycol – *p*-toluenesulfonyl chloride goes more likely via spinodal decomposition mechanism [27].

It is known that texture and morphology of polymerization induced phase separation are characterized by two values: the scale of segregation and the intensity of segregation [28]. As can be seen from Fig. 3 the temperature enhancing leads to the pore numbers increasing and, consequently, to decreasing of phase separation segregation scale [28]. On the other hand, according to mass changes measurements the non-RPF fraction in FET1105-X-180 samples after PIPS at different temperatures are 20, 18 and 12 wt% for PIPS steps at 50, 60 and 70 °C, respectively. The non-RPF fraction is the calculated residuals from ethylene glycol and *p*-toluenesulfonyl chloride taking into account mass loss in pure RPF during different heat treatments (PIPS step, post-curing or pyrolysis). Strictly speaking, the non-RPF fraction can differ from calculated values since the resol resin can behave differently in FET1105 than in pure state. The results obtained indicate that less pore-forming and catalyst molecules are trapped inside cured polymer matrix and the thermoset enriched phases have probably less content of non-RPF molecules when PIPS temperature increases. Thus, the PIPS temperature increasing probably results in the increase of the segregation intensity.

4.3. *The study of pyrolysis and pyrolysis products*

The heating of the samples after post-curing to 800 °C leads to

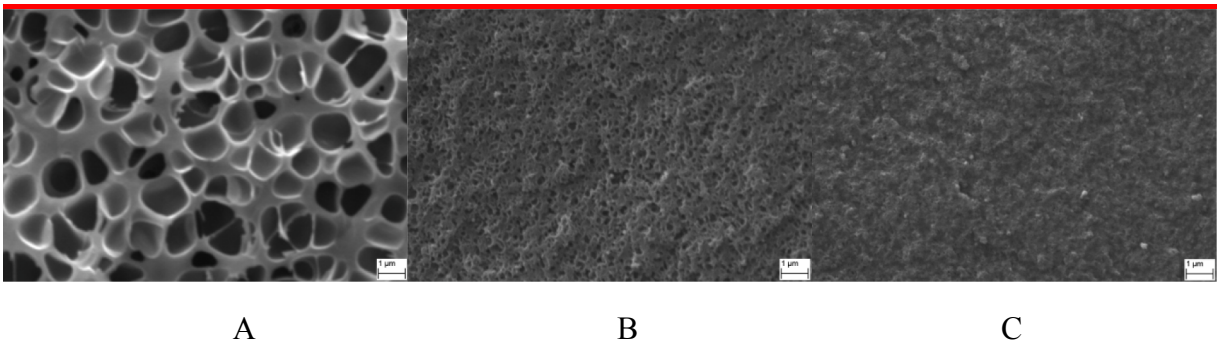

Fig. 5. Scanning electron microscopy images of the samples after post-curing and pyrolysis (× 20000): A – PIPS at 50 °C (FET1105-50-180); B – PIPS at 60 °C (FET1105-60-180); C – PIPS at 70 °C (FET1105-70-180).

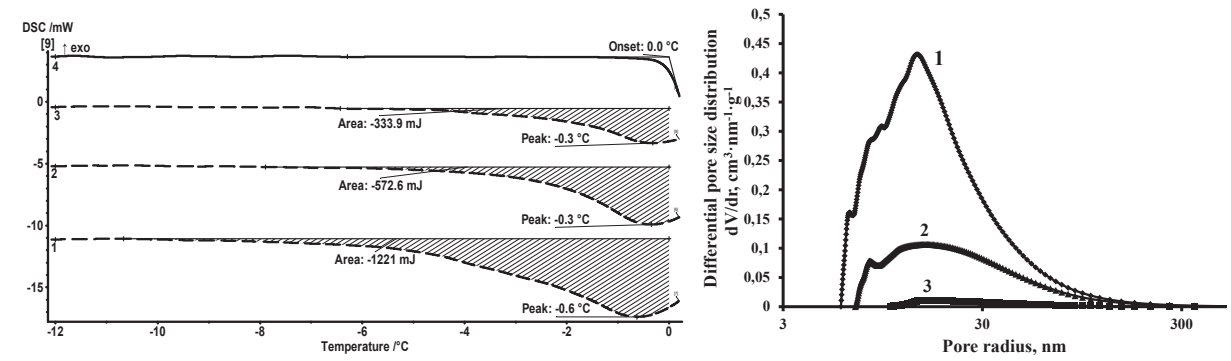

Fig. 6. DSC-curves of water melting in the water-saturated samples (A) and differential pore sizes distribution curves of the samples (B): 1 – FET1105-70-180; 2 - FET1105-60-180; 3 - FET1105-50-180; 4 – bi-distilled water.

stepwise mass loss and linear shrinkage (Fig. 4), moreover the calculated in the approximation of isotropic shrinkage relative density after some fluctuations becomes about 19% higher and 3% lower than the density before pyrolysis for RPF-90-180 and FET1105-60-180, respectively.

The initial (up to 180 °C) mass loss of the sample after post-curing at 180 °C for 6 h can be related with releasing of water and non-RPF products mixture which was trapped inside the massive sample (3 g) and became available during the cutting of the sample from the middle for thermogravimetry measurement (13 mg). Moreover, it should be noted, that according to mass balance, there was still 18 wt% of non-RPF products in the massive FET1105-60-180 sample. On the other hand the mass loss of the small sample from the middle of massive FET1105-60-180 sample under the heating to 330 °C is accompanied with mass loss of 29% while the cured resol resin RPF-90-180 losses only 2,5%.

It should be noted that the samples of the same initial chemical nature, but which were post-cured immediately after gelation, tend to densify by ~50% during pyrolysis step [19]. This observation emphasizes that sufficient PIPS time (more than only gel-time) is urgent for the formation of stable to pyrolysis porous structure.

The SEM images of the samples after pyrolysis are presented in Fig. 5.

As can be seen from Figs. 3 and 5, the pore structures after pyrolysis changed slightly: the pores broadened, but the carbon walls thinned. The thinning of carbon walls, especially for the cases of samples with low-temperature PIPS step, is probably explained by evolution of trapped non-RPF products.

The method of thermoporometry was used to obtain the pore size distribution of the samples obtained. The method of thermoporometry is based on decreasing of melting point with decreasing of sample size according to Gibbs-Thomson equation [29]. To minimize the influence of water admixtures the subtraction results of DSC-sample curves and DSC-water curve were used for calculation. The DSC-curves used for calculation are presented in Fig. 6A. The differential pore size distribution curves calculated according to procedure described in Ref. [29] are presented in Fig. 6B. The coefficients used for calculation were: $dT/dt = 1$ K/min (0.01667 K/s), $2K = 52$ nm °C, $\delta = 0.8$ nm [30]. The dependencies of ice density and melting enthalpy on temperature were used in accordance with [31].

As one can see from Fig. 6B the increasing of PIPS temperature causes the increasing of mesopores cumulative volume. It should be noted that during heating of the sample FET1105-X-180 in the temperature range of 250–320 °C, the 1,4-dioxane is the main volatile product with dipole moment despite water and carbon dioxide. The 1,4-dioxane formation during heating of the sample at the temperatures much higher than 1,4-dioxane boiling point (101 °C) can be probably explained by acid-catalyst depolymerization of olygoethylene glycol formed in the system during PIPS step and post-curing. The formation of 1,4-dioxane and tetraethylene glycol can be seen from the results of pyrolysis gas chromatography mass spectrometry (Py-GCMS) (Fig. 7). Peak at retention time of 2,5 min (Fig. 7B) corresponds to 1,4-dioxane (Fig. 7C) and peak at 8,9 min (Fig. 7D) – tetraethylene glycol (Fig. 7E). The peaks at retention time between 5 and 8 min are interaction products of ethylene glycol.

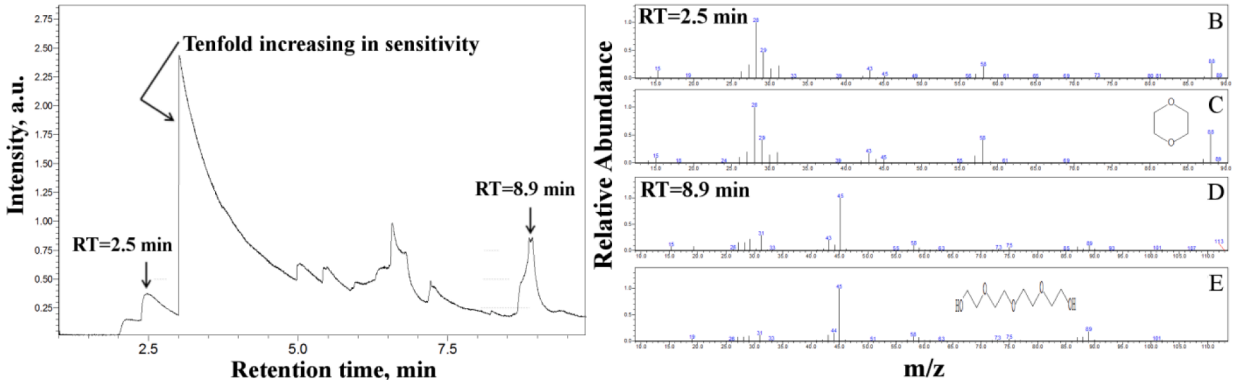

Fig. 7. Pyrolysis-GC/MS chromatogram of the FET1105-50-180 at 300 °C (A) and the mass-spectra of peak at retention time 2,5 min (B), peak at retention time 8,9 min (D), 1,4-dioxane (C) and tetraethylene glycol (E).

It is known that increasing of polyethylene glycol content and its molecular weight after phenol-formaldehyde blend pyrolysis causes the increasing of mesopores content [32]. Thus, it can be suggested that increased content of mesopores in the samples with higher PIPS step temperature can be explained and by olygoethylene glycol formation inside phenol-formaldehyde matrix.

5. Conclusion

The pore formation during polymerization induced phase separation (PIPS), post-curing and pyrolysis processes in the system resol phenol-formaldehyde resin/ethylene glycol/p-toluene sulfonyl chloride was studied by thermal analysis methods, pyrolysis gas chromatography mass spectrometry and electron microscopy. It was shown that addition of ethylene glycol and p-toluene sulfonyl chloride leads to increasing of reaction order of phenol-formaldehyde curing. It was shown that PIPS temperature increasing result in decreasing of phase separation segregation scale and increasing of macropores sizes. The PIPS temperature increasing also leads to increasing of phase separation intensity and cumulative volume of mesopores. The increased cumulative volume of mesopores is suggested to be a result of olygoethylene glycol formation. It was shown, that the main pore structure and morphology was formed during PIPS step. Insufficient PIPS time causes the formation of structures, which collapses during pyrolysis conditions.

Acknowledgements

The reported study was funded by RFBR (Russian Foundation for Basic Research) according to the research project No. 17-03-01163.

References

[1] E.N. Kablov, D.V. Grashchenkov, N.V. Isaeva, S.St Solntsev, Perspective high-temperature ceramic composite materials, Russ. J. Gen. Chem. 81 (2011) 986–991. https://doi.org/10.1134/S107036321105029X.
[2] E.N. Kablov, D.V. Grashchenkov, N.V. Isaeva, S.S. Solntsev, V.G. Sevast'yanov, Glass and ceramics based high-temperature composite materials for use in aviation technology, Glass Ceram. 69 (2012) 109–112. https://doi.org/10.1007/s10717-012-9425-1.
[3] S.V. Zhitnyuk, Oxygen-free ceramic materials for the space technics (review), VIAM works 68 (2018) 81–88. https://doi.org/10.18577/2307-6046-2018-0-8-81-88.
[4] D.V. Grashchenkov, M.L. Vaganova, N.E. Shchyogoleva, A.S. Chainikova, YuE. Lebedeva, High-temperature Glass Crystal Material of Barium Aluminosilicate Structure, Received Using Sol-Gel of Synthesis and Composite Materials on its Basis, Aviation Materials and Technologies. S, 2017, pp. 290–305. https://doi.org/10.18577/2071-9140-2017-0-S-290-305.
[5] E.P. Simonenko, N.P. Simonenko, A.V. Derbenev, V.A. Nikolaev, D. V. Grashchenkov, V.G. Sevastyanov, E.N. Kablov, N.T. Kuznetsov, Synthesis of nanocrystalline silicon carbide using the sol-gel technique, Russ. J. Inorg. Chem. 58 (2013) 1143–1151. https://doi.org/10.1134/S0036023613100215.
[6] Department of Defense Handbook Composite Materials Handbook Volume 5, 2002. Ceramic matrix composites.
[7] V.A. Prokofiev, O.Ju Sorokin, M.L. Vaganova, YuE. Lebedeva, High-temperature functionally graded material fabricated via reactive alloy infiltration, VIAM works 71 (2018) 45–53. https://doi.org/10.18577/2307-6046-2018-0-11-45-53.
[8] T. Horikawa, K. Ogawa, K. Mizuno, J. Hayashi, K. Muroyama, Preparation and characterization of the carbonized material of phenol–formaldehyde resin with addition of various organic substances, Carbon 41 (2003) 465–472. https://doi.org/10.1016/S0008-6223(02)00352-4.
[9] K. Inomata, Y. Otake, Activation-free preparation of porous carbon by carbonizing phenolic resin containing pore-forming substance, Energy Procedia 14 (2012) 626–631. https://doi.org/10.1016/j.egypro.2011.12.986.
[10] H. Byun, G. Nam, Y.-M. Rhym, S.E. Shim, Phenol/formaldehyde-derived macroporous carbon foams prepared with aprotic ionic liquid as liquid template, Carbon Lett. 13 (2012) 94–98. https://doi.org/10.5714/CL.2012.13.2.094.
[11] G. Nam, S. Choi, H. Byun, Y.-M. Rhym, S.E. Shim, Preparation of macroporous carbon foams using a polyurethane foam template replica method without curing step, Macromol. Res. 21 (2013) 958–964. https://doi.org/10.1007/s13233-013-1114-6.
[12] H. Nishihara, S.R. Mukai, H. Tamon, Preparation of resorcinol–formaldehyde carbon cryogel microhoneycombs, Carbon 42 (2004) 885–901. https://doi.org/10.1016/j.carbon.2004.01.075.
[13] M. Wang, Y. Yu, X. Wu, S. Li, Polymerization induced phase separation in poly (ether imide)-modified epoxy resin cured with imidazole, Polymer 45 (2004) 1253–1259. https://doi.org/10.1016/j.polymer.2003.12.037.
[14] S. Xu, G. Qiao, H.D. Wang, D. Li, T. Lu, Preparation of mesoporous carbon derived from mixtures of phenol-formaldehyde resin and ethylene glycol, Mater. Lett. 62 (2008) 3716–3718. https://doi.org/10.1016/j.matlet.2008.04.037.
[15] G. Zhang, Z. Xiao, G. Qiao, Preparation and mechanism of interconnected mesoporous carbon monoliths from phenolic resin/ethylene glycol mixtures, Key Eng. Mater. 512–515 (2012) 403–406. https://doi.org/10.4028/www.scientific.net/KEM.512-515.403.
[16] G. Zhang, G. Liu, Z. Shi, G. Qiao, Dynamics of spinodal decomposition coupled with chemical reaction in thermosetting phenolformaldehyde resin-based solutions and its application in monolithic porous materials, RSC Adv. 4 (2014) 7068–7078. https://doi.org/10.1039/C3RA46490C.
[17] ASTM E2041-08. Standard Test Method for Estimating Kinetic Parameters by Differential Scanning Calorimeter Using the Borchardt and Daniels Method.
[18] R.A. Satdinov, S.E. Istyagin, E.A. Veshkin, Analysis of the temperature-time parameters mode curing PCM with specified characteristics, VIAM works 51 (2017) 85–94. https://doi.org/10.18577/2307-6046-2017-0-3-9-9.
[19] M.A. Khaskov, A.M. Shestakov, S.D. Sinyakov, O.Yu Sorokin, A.I. Gulyaev, I. V. Zelenina, Thermo-kinetic researches for formation of carbon matrix - precursor for reactive infiltration with melt, Izv. Vyssh. Uchebn. Zaved. Khim. Khim. Tekhnol. 61 (2018) 31–37. https://doi.org/10.6060/ivkkt.20186111.3y.
[20] R. Rego, P.J. Adriaensens, R.A. Carleer, J.M. Gelan, Fully quantitative carbon-13 NMR characterization of resol phenol–formaldehyde prepolymer resins, Polymer 45 (2004) 33–38. https://doi.org/10.1016/j.polymer.2003.10.078.
[21] R. Ding, Y. He, X. Wang, J. Xu, Y. Chen, M. Feng, C. Qi, Treatment of alcohols with tosyl chloride does not always lead to the formation of tosylates, Molecules 16 (2011) 5665–5673. https://doi.org/10.3390/molecules16075665.
[22] J. Wang, M.-P.G. Laborie, M.P. Wolcott, Comparison of model-fitting kinetics for predicting the cure behavior of commercial phenol–formaldehyde resins, J. Appl. Polym. Sci. 105 (2007) 1289–1296. https://doi.org/10.1002/app.24855.
[23] S. Vyazovkin, A.K. Burnham, J.M. Criado, L.A. Pérez-Maqueda, C. Popescu, N. Sbirrazzuoli, ICTAC Kinetics Committee recommendations for performing kinetic computations on thermal analysis data, Thermochim. Acta 520 (2011) 1–19. https://doi.org/10.1016/j.tca.2011.03.034.
[24] L.T. Manzione, J.K. Gillham, C.A. McPherson, Rubber-modified epoxies. I. Transitions and morphology, J. Appl. Polym. Sci. 26 (1981) 889–905. https://doi.org/10.1002/app.1981.070260313.
[25] S. Swier, B. Van Mele, In situ monitoring of reaction-induced phase separation with modulated temperature DSC: comparison between high-Tg and low-Tg modifiers, Polymer 44 (2003) 2689–2699. https://doi.org/10.1016/S0032-3861(03)00138-1.
[26] M.A. Khaskov, The using of thermal analysis methods for the construction of isothermal transformation diagrams of thermosets, Polym. Sci. B 59 (2017) 51–61. https://doi.org/10.1134/S1560090417010080.
[27] P.C. Fife, Models for phase separation and their mathematics, Electron. J. Differ. Equ. 2000 (2000) 1–26.
[28] J. Oh, A.D. Rey, Computational simulation of polymerization-induced phase separation under a temperature gradient, Comput. Theor. Polym. Sci. 11 (2001) 205–217. https://doi.org/10.1016/S1089-3156(00)00013-1.
[29] J. Riikonen, J. Salonen, V.-P. Lehto, Utilising thermoporometry to obtain new insights into nanostructured materials – review part 2, J. Therm. Anal. Calorim. 105 (2011) 823–830. https://doi.org/10.1007/s10973-011-1337-8.
[30] P. Veselá, J. Riikonen, T. Nissinen, V.-P. Lehto, Václav Slovák, Optimisation of thermoporometry measurements to evaluate mesoporous organic and carbon xero-, cryo- and aerogels, Thermochim. Acta 621 (2015) 81–89. https://doi.org/10.1016/j.tca.2015.10.016.
[31] B. Charmas, J. Skubiszewska-Zięba, Application of differential scanning calorimetry to study porous structure of hydrothermally modified silicas, J. Therm. Anal. Calorim. 129 (2017) 23–32. https://doi.org/10.1007/s10973-017-6126-6.
[32] X. Zhang, H. Hu, Y. Zhu, S. Zhu, Carbon molecular sieve membranes derived from phenol formaldehyde novolac resin blended with poly(ethylene glycol), J. Membr. Sci. 289 (2007) 86–91. https://doi.org/10.1016/j.memsci.2006.11.047.